



Published in final edited form as:

*J Otolaryngol Head Neck Surg.* 2010 April ; 39(2): 150–156.

## Optical Coherence Tomography of the Larynx Using the Niris System

**Marc Rubinstein, MD, Esther L. Fine, MD, Ali Sepehr, MD, William B. Armstrong, MD, Roger L. Crumley, MD, MBA, Jason H. Kim, MD, Zhongping Chen, PhD, and Brian J.F. Wong, MD, PhD**

Marc Rubinstein: Department of Otolaryngology–Head and Neck Surgery and Beckman Laser Institute and Medical Clinic; Esther L. Fine, Ali Sepehr, William B Armstrong, Roger L. Crumley, and Jason H. Kim: Department of Otolaryngology–Head and Neck Surgery; Zhongping Chen: Beckman Laser Institute and Medical Clinic, and Department of Biomedical Engineering; and Brian J.F. Wong: Department of Otolaryngology-Head and Neck Surgery and Beckman Laser Institute and Medical Clinic and Department of Biomedical Engineering, University of California Irvine, Irvine, California.

### Abstract

**Objectives**—To present our experience using the first commercially available optical coherence tomography (OCT) device for use in the head, neck, and upper aerodigestive tract and to determine the feasibility and efficacy of this system in comparison with our previous experience using other research OCT systems.

**Methods**—Using the Niris OCT imaging system (Imalux, Cleveland, OH), we obtained OCT images of benign and premalignant laryngeal disease in 33 patients undergoing surgical head and neck endoscopy. This imaging system has a spatial depth resolution of 10 to 20  $\mu\text{m}$  and a depth scanning range of 2.2 mm, obtaining images of 200  $\times$  200 pixels at a maximum frame rate of 0.7 Hz. The scanning mechanism of the device is located at the distal end of a flexible probe that is placed in contact or near-contact with the area of interest. The tip of the probe was inserted through a rigid laryngoscope, and still images were obtained.

**Results**—OCT images of arytenoids, aryepiglottic folds, piriform sinus, epiglottis, and true and false vocal cords were obtained. In patients whose OCT images were taken from normal tissue, the normal microstructures were clearly identified, as well as disruption of the latter in malignant pathologies.

**Conclusions**—The device can easily be incorporated into the operating room and requires minimal set-up and staff to operate. OCT imaging with this device potentially offers an efficient, quick, and reliable imaging modality in guiding surgical biopsies, intraoperative decision making, and therapeutic options of various laryngeal pathologies and premalignant disease.

### Keywords

endoscopy; imaging; larynx; optical coherence tomography; otolaryngology; vocal folds

---

© 2010 The Canadian Society of Otolaryngology-Head & Neck Surgery

Address reprint requests to: Brian J.F. Wong, MD, PhD, Beckman Laser Institute and Medical Clinic, University of California Irvine, 1002 Health Sciences Rd, Irvine, CA 92612; bjwong@uci.edu.

This work was presented at the Western Section of the Triological Society Meeting, January 29–31, 2009, Las Vegas, NV.

Financial disclosure of reviewers: None reported.

Optical coherence tomography (OCT) is an emerging imaging modality that combines a low-coherence light source and an interferometer to produce cross-sectional high-resolution images of living tissues.<sup>1</sup> OCT works analogously to ultrasonography but instead of sound uses near-infrared light to discern variation in tissue optical properties. Clinical OCT devices have an axial resolution of approximately 10  $\mu\text{m}$  and a maximum depth penetration of 2 to 3 mm, although 1 to 2 mm is more typical because most biologic tissues are turbid.<sup>2</sup> This technology has been widely used in ophthalmology for examination of the retina, cornea, and macula<sup>3–5</sup> and as a guide in cataract surgery.<sup>6</sup> OCT has been evaluated in other specialties, including dermatology, cardiology, pulmonology, gastroenterology, urology, and neurology, although primarily using research OCT systems designed and constructed by specialists in photonic technologies at academic medical centres.<sup>7–12</sup>

In the head, neck, and upper aerodigestive tract, clinical OCT has focused on examination of the larynx, with one goal: to distinguish benign from microinvasive cancer that has violated the integrity of the basement membrane (BM).<sup>2,13–18</sup> Some work has focused on using OCT to perform image-guided therapy of the larynx, although the results have been mixed.<sup>19</sup> It has also been used coupled to a surgical microscope, allowing hands-free OCT simultaneously with microscopic visualization of the vocal cords.<sup>20</sup> More recently, we pioneered the use of OCT to image both the neonatal and the pediatric airway with the aim of examining changes in the subglottis following prolonged intubation.<sup>21,22</sup> OCT has also been used to image the middle ear and thyroid gland.<sup>23–26</sup> The oral cavity has been studied comprehensively using OCT and is reviewed elsewhere.<sup>24,25,27–33</sup>

Outside of ophthalmology, most clinical OCT studies have involved the use of systems designed and built by research groups focused on enhancing the resolution, image acquisition rates, and functionality of this nascent imaging modality. Until recently, there has not been a commercially available turnkey OCT system for use in the head and neck, and most studies to date have used research devices designed and constructed in university optics laboratories.

At University of California Irvine, we have had an active OCT research program at the Beckman Laser Institute and Medical Clinic for over 15 years, with over 7 years of clinical experience on OCT imaging in the head and neck in human subjects. Our investigations to date have used only OCT systems designed and constructed in our laboratories. The objective of this study was to present our experience with using the first commercially available OCT device designed to image the larynx among other applications and to compare its use with our previous experience in over 200 patients using research OCT systems.

## Materials and Methods

### Patient Population

OCT imaging was performed in 33 patients undergoing upper aerodigestive tract endoscopy under general anesthesia, under the aegis of the Institutional Review Board at the University of California Irvine. Two subjects were imaged twice during two separate operations. Twenty-one patients (64%) were male and 12 patients (36%) were female. The average age was 53 years (range 18–86 years). Imaging generally required 3 to 5 minutes of additional surgical time.

### OCT System

A commercially available clinical imaging system (Niris, Imalux Corporation, Cleveland, OH) was used to examine each patient. This portable time-domain OCT system<sup>34</sup> uses a low-coherence near-infrared light source to acquire real-time images of 200  $\times$  200 pixels at a maximum frame rate of 0.7 Hz. The spatial depth resolution of the system is 10 to 20  $\mu\text{m}$ , with

a depth scanning range of 2.2 mm. In practice, owing to the turbidity of living tissues, scanning depth is only about 1.5 mm. The lateral resolution is 25  $\mu\text{m}$ , with a lateral scanning range of 1.5 to 2.5 mm. In OCT systems, lateral resolution is diffraction limited, whereas axial resolution depends on the coherence length of the light sources. It uses a 2.7 mm diameter reusable flexible probe to obtain the images. To the user, the probe appears as a single, compact instrument; however, it encases a single-mode optical fibre, which is scanned back and forth within by a solenoid.

### Intraoperative Imaging

After exposing the larynx using a surgical laryngoscope with suspension, the probe was inserted through the laryngoscope using a modified suction handpiece to allow accurate placement of the probe tip on the area of interest (Figure 1). Under microscopic or rigid telescope (eg, a Hopkins rod) guidance, the probe tip was placed in gentle or near-contact with the region of interest. OCT images were acquired from the normal laryngeal tissue, the site of the pathology, and in transition zones in the case of potential cancers. In most of the patients, still images of the lesion were acquired using conventional digital imaging, which also aided in providing a record of the probe position.

### OCT Image Analysis

Images from the laryngeal subsites were obtained. Images were then arranged by anatomic site and then subdivided into the following three categories: (a) normal tissue, (b) benign lesions, and (c) malignant lesions.

### Results

OCT images of the true vocal cords (TVCs) were obtained in 29 of the 33 patients. OCT images were also obtained from the false vocal cords (FVCs), arytenoids, aryepiglottic fold, piriform sinus, and epiglottis. In patients whose OCT images were taken from normal tissue, the normal microstructures were clearly identified.

The following images represent the features, disorders, and pathology that were imaged in which the epithelium and lamina propria (LP) and other microstructures were clearly identified, as well as the demarcation between the LP and epithelium, which is the locus of the BM. Figure 2 is a typical OCT image of the TVC, with identification of the thin, translucent appearance of the stratified squamous epithelium (SSE), the integrity of the BM, and the underlying LP. This image can be compared with an image of a TVC with scar tissue caused by previous operations, showing a thickening of the LP as well as the overlying SSE (Figure 3). Figure 4 is an image of an invasive carcinoma of the TVC. The integrity of the BM is disrupted, which is the most important parameter of invasion. In Figure 5, a transition zone between normal tissue and an invasive carcinoma infiltrating through the BM is clearly shown in a false vocal cord. This image can be compared with a normal FVC where the BM is clearly intact (Figure 6).

The presence cartilage and glandular structures are identified in the epiglottis (Figure 7). A remnant scar caused by previous surgeries of the epiglottis as well as some glandular structures can be seen in Figure 8. The normal microstructure of the aryepiglottic fold can be seen in Figure 9, where no glandular structures are identified.

### Discussion

We present our experience imaging normal, benign, and pathologic conditions in the larynx using the first commercial OCT device designed for use in head and neck endoscopic

applications. Currently, other commercially available OCT devices are available for use in other medical fields, such as ophthalmology,<sup>35</sup> gastroenterology,<sup>36</sup> and cardiology<sup>37</sup>; however, these systems do not work in otolaryngology. Other non-commercially available OCT systems, which have a higher resolution and scanning rate, have been previously reported and are summarized in Table 1; however, none of these systems have been used in head and neck applications.<sup>38–40</sup>

Present diagnostic imaging, including magnetic resonance imaging, computed tomography, and ultrasonography, offers 1 mm tissue resolution at best and thus is of limited use in very superficial laryngeal lesions.<sup>18</sup> OCT has the unique capability of producing high-resolution images of 10 to 20  $\mu\text{m}$ , which are useful to assess very thin structures, such as the surface of the larynx. We concur with the results published by Shakhov and colleagues, who found that a definitive diagnosis of laryngeal lesions requires tissue biopsy, and this carries the risks of compromising the airway and potentially causing a scar formation.<sup>19</sup>

We have found that the Niris device provides images of sufficient quality such that normal structures can be easily differentiated from benign or malignant lesions. This system was extensively used by Kraft and colleagues in a large number of patients and for a broad list of disorders.<sup>18</sup> They concluded that this device is a useful complement in the diagnosis of different laryngeal diseases; however, their group does not have extensive experience with cutting-edge OCT technology such as exists in our centre and others.

When comparing this system with the ones previously used,<sup>2,13,14</sup> the Niris has limited lateral resolution, a slower frame rate, and a decreased depth of imaging. The scanning mechanism for the Niris is at the tip, and the optical elements move right to left across the target region in the tissue. Previous devices constructed by our group and others obtained cross-sectional images with the probe tip moving in and out of the probe long axis. Left to right imaging allows easier targeting of regions of interest on the vocal cords and the surrounding structures. Benign abnormalities demonstrated unique OCT characteristics, which allowed them to be differentiated from both normal tissues and malignancies.

OCT has limited capabilities in imaging large and bulky laryngeal lesions because the BM cannot be consistently identified, making it difficult to evaluate BM infiltration and to distinguish between benign and malignant lesions. Thus, OCT has its greatest potential value in examining superficial and subtle lesions and disease processes. This device has limited utility for imaging bulky lesions but might be useful to evaluate surgical margins following the resection of a bulky lesion and as an adjunctive technology for use in transoral laser microsurgery.

This system is an easy to use device, is portable, requires a single operator, and takes approximately 3 to 5 minutes to set up. Although the image quality is limited relative to previously described research devices,<sup>2,13,14</sup> laryngeal microstructures, such as the BM, LP, epithelium, glands, and capillaries, can be identified, still making this device valuable for select applications.

OCT has potential use as a complementary tool for diagnosing various laryngeal pathologies. It can be a great asset in the operating room in guiding surgical biopsies, decreasing the necessity of removing broader surgical margins, and intraoperative decision making.

## Acknowledgments

Financial disclosure of authors: This work was supported by the National Institutes of Health (DC 006026, CA 91717, EB 00293, RR 01192, RR00827), Flight Attendant Medical Research Institute (32456), State of California Tobacco

Related Disease Research Program (12RT-0113), Air Force Office of Scientific Research (F49620\_00\_1\_0371), and the Arnold and Mabel Beckman Foundation.

## References

1. Huang D, Swanson EA, Lin CP, et al. Optical coherence tomography. *Science* 1991;254:1178–1181. [PubMed: 1957169]
2. Wong BJ, Jackson RP, Guo S, et al. In vivo optical coherence tomography of the human larynx: normative and benign pathology in 82 patients. *Laryngoscope* 2005;115:1904–1911. [PubMed: 16319597]
3. Voo I, Mavrofrides EC, Puliafito CA. Clinical applications of optical coherence tomography for the diagnosis and management of macular diseases. *Ophthalmol Clin North Am* 2004;17:21–31. [PubMed: 15102511]
4. Costa RA, Skaf M, Melo LA Jr, et al. Retinal assessment using optical coherence tomography. *Prog Retin Eye Res* 2006;25:325–353. [PubMed: 16716639]
5. Feng Y, Simpson TL. Corneal, limbal, and conjunctival epithelial thickness from optical coherence tomography. *Optom Vis Sci* 2008;85:E880–E883. [PubMed: 18772715]
6. Schallhorn JM, Tang M, Li Y, et al. Optical coherence tomography of clear corneal incisions for cataract surgery. *J Cataract Refract Surg* 2008;34:1561–1565. [PubMed: 18721720]
7. Gambichler T, Moussa G, Sand M, et al. Applications of optical coherence tomography in dermatology. *J Dermatol Sci* 2005;40:85–94. [PubMed: 16139481]
8. Patwari P, Weissman NJ, Boppart SA, et al. Assessment of coronary plaque with optical coherence tomography and high-frequency ultrasound. *Am J Cardiol* 2000;85:641–644. [PubMed: 11078281]
9. Hanna N, Saltzman D, Mukai D, et al. Two-dimensional and 3-dimensional optical coherence tomographic imaging of the airway, lung, and pleura. *J Thorac Cardiovasc Surg* 2005;129:615–622. [PubMed: 15746746]
10. Bouma BE, Tearney GJ, Compton CC, Nishioka NS. High-resolution imaging of the human esophagus and stomach in vivo using optical coherence tomography. *Gastrointest Endosc* 2000;51 (4 Pt 1):467–474. [PubMed: 10744824]
11. Zagaynova EV, Streltsova OS, Gladkova ND, et al. In vivo optical coherence tomography feasibility for bladder disease. *J Urol* 2002;167:1492–1496. [PubMed: 11832776]
12. Jafri MS, Farhang S, Tang RS, et al. Optical coherence tomography in the diagnosis and treatment of neurological disorders. *J Biomed Opt* 2005;10:051603. [PubMed: 16292951]
13. Armstrong WB, Ridgway JM, Vokes DE, et al. Optical coherence tomography of laryngeal cancer. *Laryngoscope* 2006;116:1107–1113. [PubMed: 16826043]
14. Sepehr A, Armstrong WB, Guo S, et al. Optical coherence tomography of the larynx in the awake patient. *Otolaryngol Head Neck Surg* 2008;138:425–429. [PubMed: 18359348]
15. Burns JA, Zeitels SM, Anderson RR, et al. Imaging the mucosa of the human vocal fold with optical coherence tomography. *Ann Otol Rhinol Laryngol* 2005;114:671–676. [PubMed: 16240928]
16. Bibas AG, Podoleanu AG, Cucu RG, et al. Optical coherence tomography in otolaryngology: original results and review of the literature. *Proc SPIE* 2004;5312:190–195.
17. Shakhov A, Terentjeva A, Gladkova ND, et al. Capabilities of optical coherence tomography in laryngology. *Proc SPIE* 1999;3590:250–260.
18. Kraft M, Glanz H, von Gerlach S, et al. Clinical value of optical coherence tomography in laryngology. *Head Neck* 2008;30:1628–1635. [PubMed: 18767182]
19. Shakhov AV, Terentjeva AB, Kamensky VA, et al. Optical coherence tomography monitoring for laser surgery of laryngeal carcinoma. *J Surg Oncol* 2001;77:253–258. [PubMed: 11473374]
20. Vokes DE, Jackson R, Guo S, et al. Optical coherence tomography-enhanced microlaryngoscopy: preliminary report of a non-contact optical coherence tomography system integrated with a surgical microscope. *Ann Otol Rhinol Laryngol* 2008;117:538–547. [PubMed: 18700431]
21. Ridgway JM, Su J, Wright R, et al. Optical coherence tomography of the newborn airway. *Ann Otol Rhinol Laryngol* 2008;117:327–334. [PubMed: 18564528]
22. Ridgway JM, Ahuja G, Guo S, et al. Imaging of the pediatric airway using optical coherence tomography. *Laryngoscope* 2007;117:2206–2212. [PubMed: 18322424]

23. Pitris C, Saunders KT, Fujimoto JG, Brezinski ME. High-resolution imaging of the middle ear with optical coherence tomography: a feasibility study. *Arch Otolaryngol Head Neck Surg* 2001;127:637–642. [PubMed: 11405861]
24. Chen SF, Lu CW, Tsai MT, et al. Oral cancer diagnosis with optical coherence tomography. *Conf Proc IEEE Eng Med Biol Soc* 2005;7:7227–7229. [PubMed: 17281947]
25. Ridgway JM, Armstrong WB, Guo S, et al. In vivo optical coherence tomography of the human oral cavity and oropharynx. *Arch Otolaryngol Head Neck Surg* 2006;132:1074–1081. [PubMed: 17043254]
26. Pantanowitz L, Hsiung PL, Ko TH, et al. High-resolution imaging of the thyroid gland using optical coherence tomography. *Head Neck* 2004;26:425–434. [PubMed: 15122659]
27. Tsai MT, Lee HC, Lee CK, et al. Effective indicators for diagnosis of oral cancer using optical coherence tomography. *Opt Express* 2008;16:15847–15862. [PubMed: 18825221]
28. Tsai MT, Lee HC, Lu CW, et al. Delineation of an oral cancer lesion with swept-source optical coherence tomography. *J Biomed Opt* 2008;13:044012. [PubMed: 19021340]
29. Colston BW Jr, Everett MJ, Da Silva LB, et al. Imaging of hard- and soft-tissue structure in the oral cavity by optical coherence tomography. *Appl Opt* 1998;37:3582–3585. [PubMed: 18273327]
30. Colston BW Jr, Everett MJ, Sathyam US, et al. Imaging of the oral cavity using optical coherence tomography. *Monogr Oral Sci* 2000;17:32–55. [PubMed: 10949834]
31. Kawakami-Wong H, Gu S, Hammer-Wilson MJ, et al. In vivo optical coherence tomography-based scoring of oral mucositis in human subjects: a pilot study. *J Biomed Opt* 2007;12:051702. [PubMed: 17994875]
32. Muanza TM, Cotrim AP, McAuliffe M, et al. Evaluation of radiation-induced oral mucositis by optical coherence tomography. *Clin Cancer Res* 2005;11:5121–5127. [PubMed: 16033826]
33. Wilder-Smith P, Jung WG, Brenner M, et al. In vivo optical coherence tomography for the diagnosis of oral malignancy. *Lasers Surg Med* 2004;35:269–275. [PubMed: 15493024]
34. van Velthoven ME, Faber DJ, Verbraak FD, et al. Recent developments in optical coherence tomography for imaging the retina. *Prog Retin Eye Res* 2007;26:57–77. [PubMed: 17158086]
35. Savini G, Zanini M, Barboni P. Influence of pupil size and cataract on retinal nerve fiber layer thickness measurements by stratus OCT. *J Glaucoma* 2006;15:336–340. [PubMed: 16865012]
36. Testoni PA, Mariani A, Mangiavillano B, et al. Intraductal optical coherence tomography for investigating main pancreatic duct strictures. *Am J Gastroenterol* 2007;102:269–274. [PubMed: 17100970]
37. Kume T, Akasaka T, Kawamoto T, et al. Assessment of coronary arterial thrombus by optical coherence tomography. *Am J Cardiol* 2006;97:1713–1717. [PubMed: 16765119]
38. Jeon MY, Zhang J, Wang Q, Chen Z. High-speed and wide bandwidth Fourier domain mode-locked wavelength swept laser with multiple SOAs. *Opt Express* 2008;16:2547–2554. [PubMed: 18542336]
39. Potsaid B, Gorczynska I, Srinivasan VJ, et al. Ultrahigh speed spectral/Fourier domain OCT ophthalmic imaging at 70,000 to 312,500 axial scans per second. *Opt Express* 2008;16:15149–15169. [PubMed: 18795054]
40. Oh WY, Yun SH, Vakoc BJ, et al. High-speed polarization sensitive optical frequency domain imaging with frequency multiplexing. *Opt Express* 2008;16:1096–1103. [PubMed: 18542183]

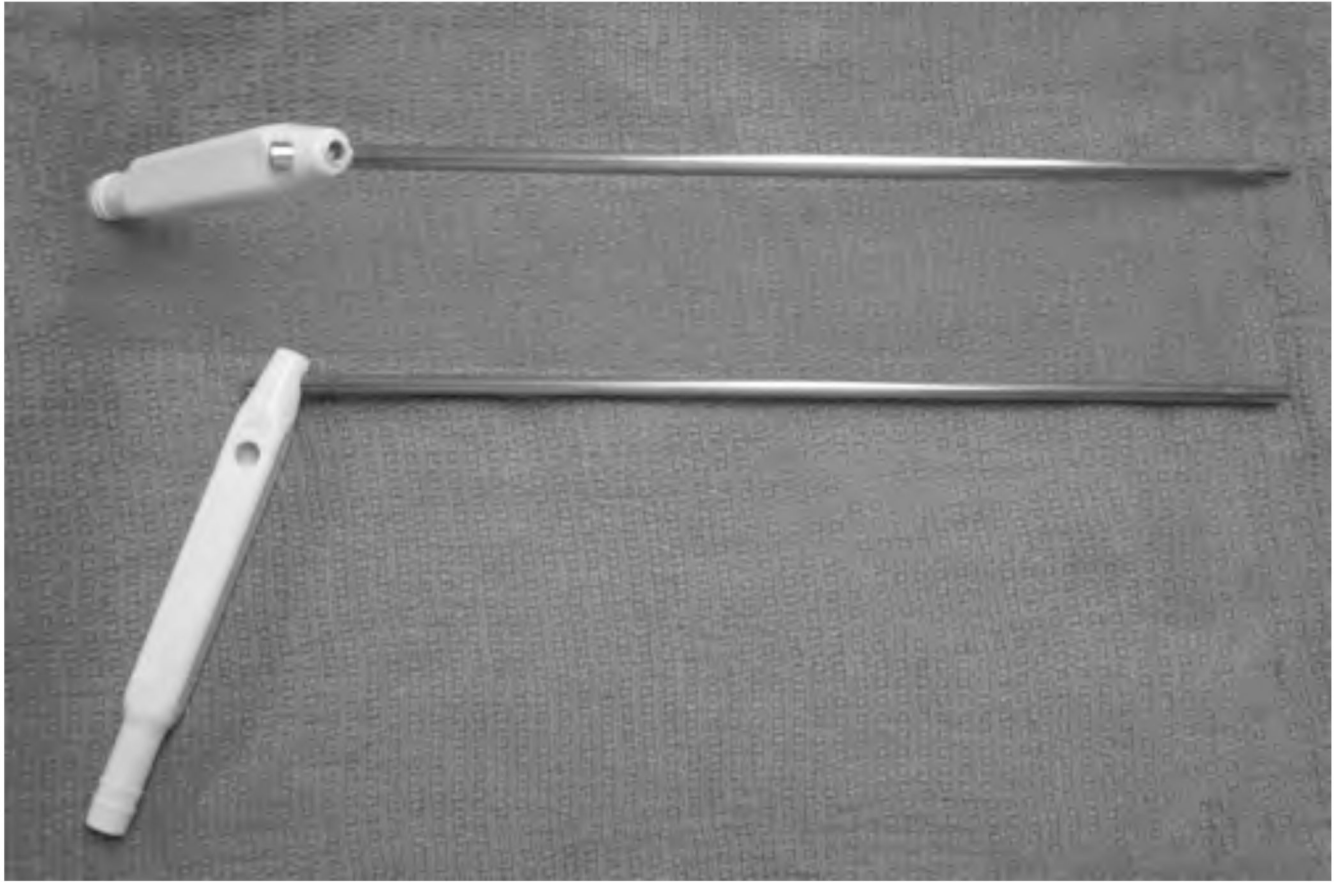


**Figure 1.**  
Specially designed device to guide the flexible probe into the larynx.

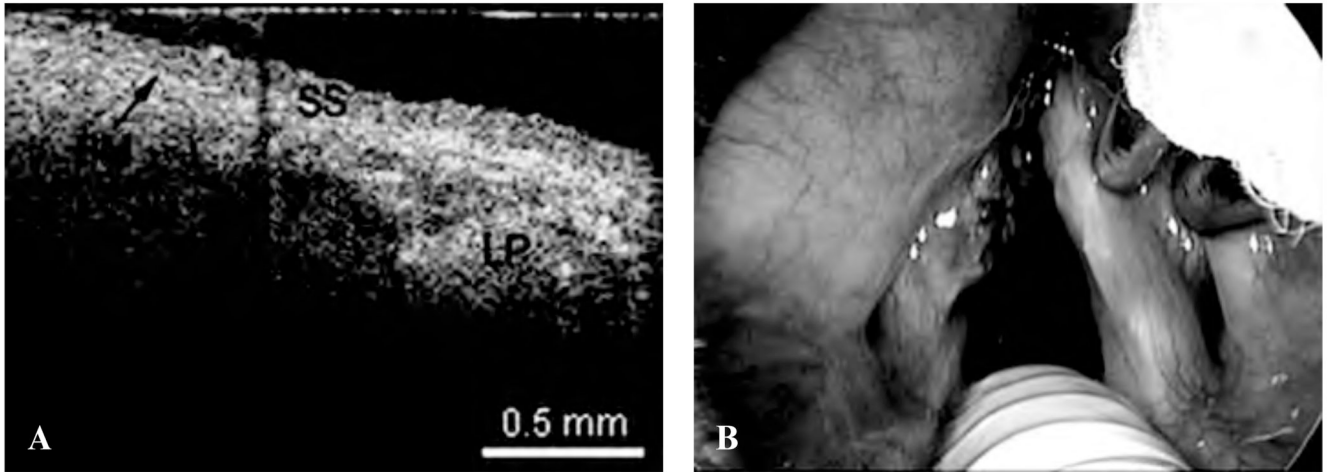


**Figure 2.**  
A, Optical coherence tomographic (OCT) image of a healthy normal true vocal cord. BM = basement membrane; LP = lamina propria; SS = stratified squamous epithelium. B, Endoscopic image showing the OCT probe being placed at the true vocal cord.



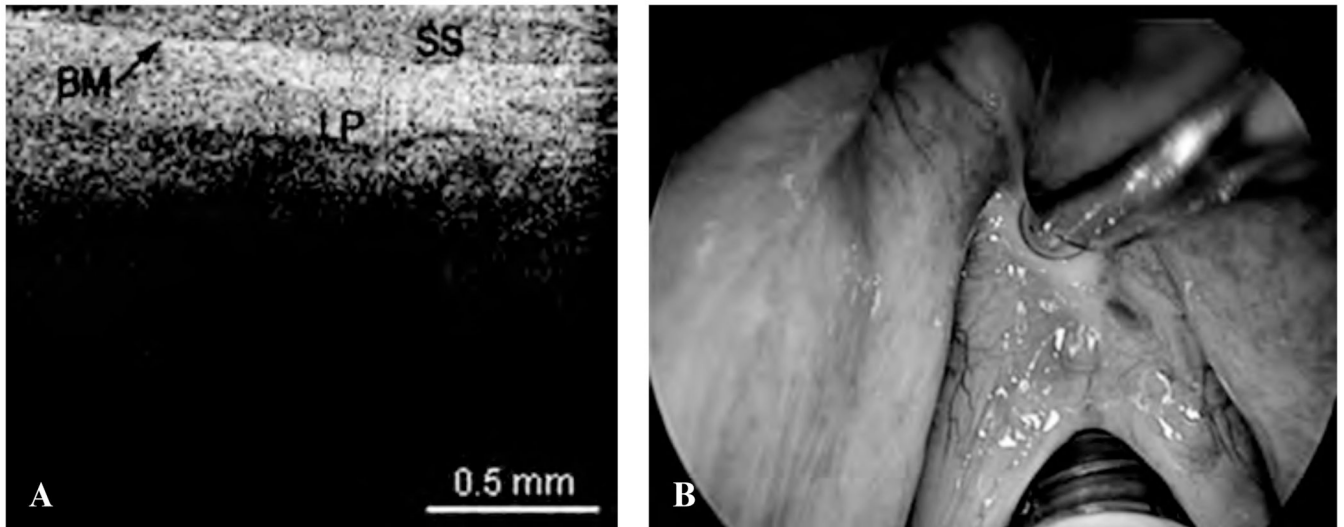


**Figure 3.**

*A*, Optical coherence tomographic (OCT) image of a true vocal cord with scar tissue and thickening of the lamina propria (LP) and stratified squamous epithelium (SS). BM = basement membrane. *B*, Endoscopic image of the OCT probe being placed at the scar tissue of the vocal cords.

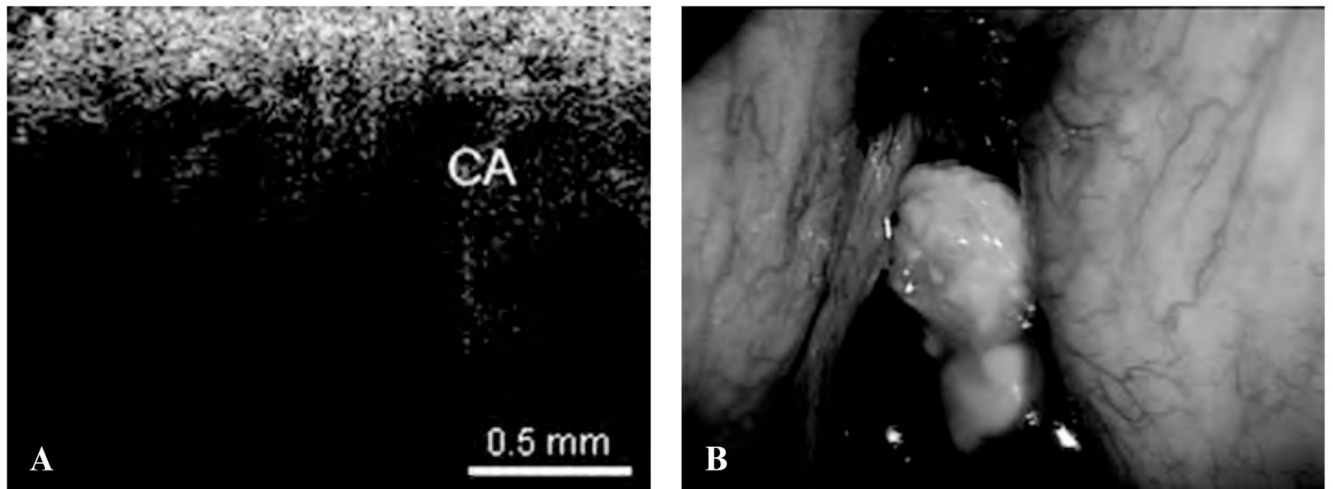


**Figure 4.**  
A, Optical coherence tomographic (OCT) image of invasive carcinoma (CA) of the true vocal cord, showing disruption and penetration through the basement membrane. B, Endoscopic image showing the invasive carcinoma of the true vocal cord.

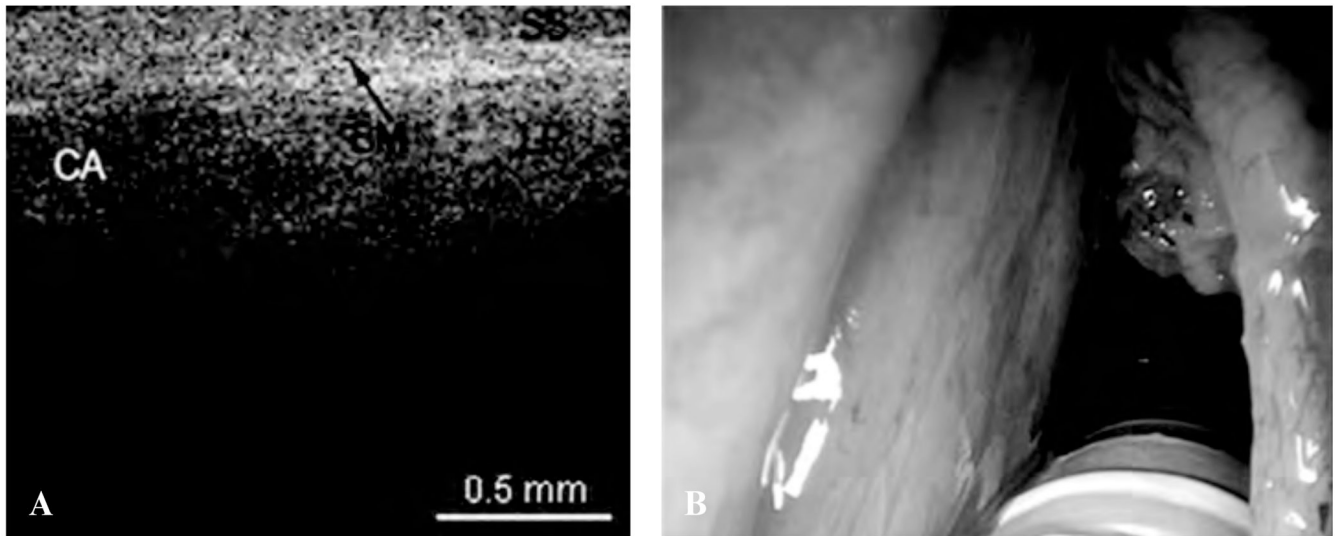


**Figure 5.**  
A, Optical coherence tomographic image of the transition zone between normal false vocal cord and invasive carcinoma (CA) invading through the basement membrane (BM). LP = lamina propria; SS = stratified squamous epithelium. B, Endoscopic image showing the false vocal cord tumor.

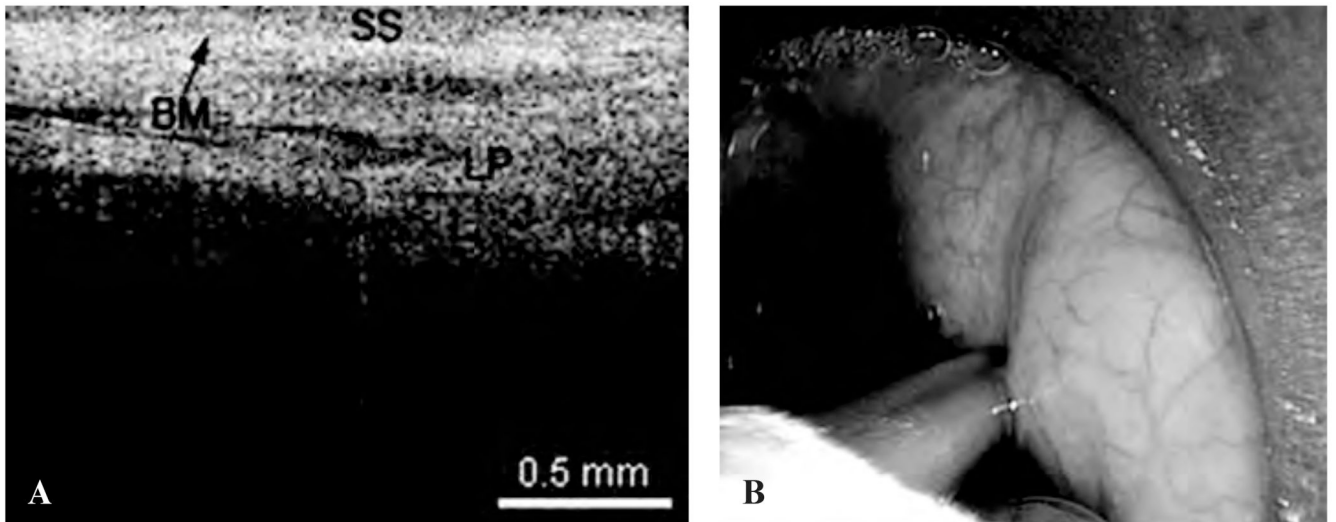


**Figure 6.**  
*A*, Optical coherence tomographic (OCT) image of a normal false vocal cord. BM = basement membrane; LP = lamina propria; SS = stratified squamous epithelium. *B*, Endoscopic image showing the OCT probe being placed at the false vocal cords.

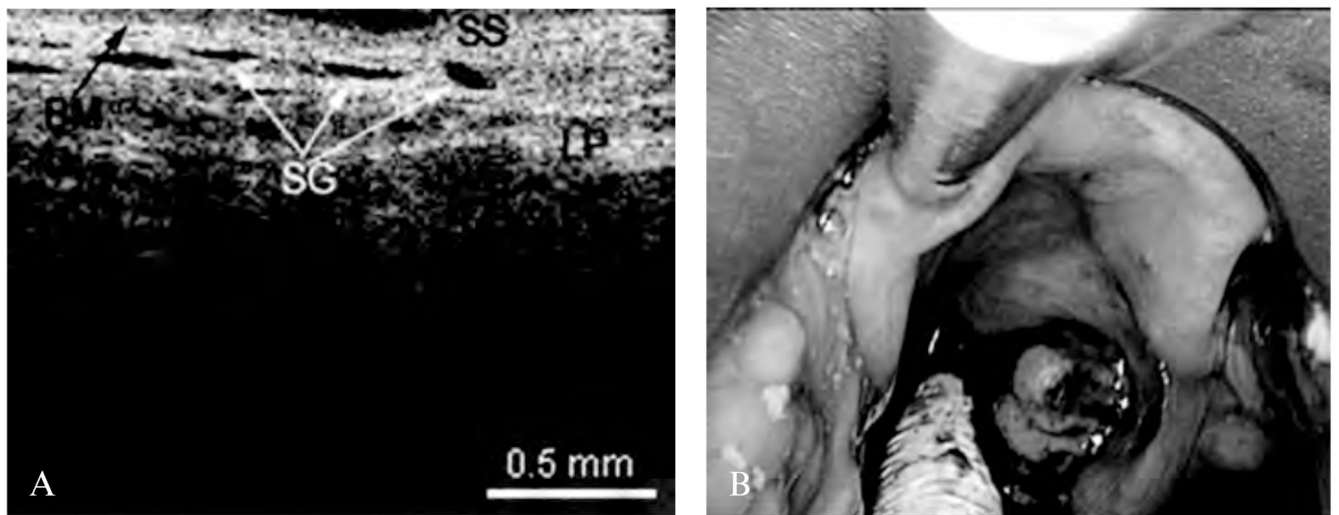


**Figure 7.**  
A, Optical coherence tomographic (OCT) image of a normal epiglottis. BM = basement membrane; LP = lamina propria; SG = seromucinous glands; SS = stratified squamous epithelium. B, Endoscopic image showing the OCT probe being placed at the epiglottis.

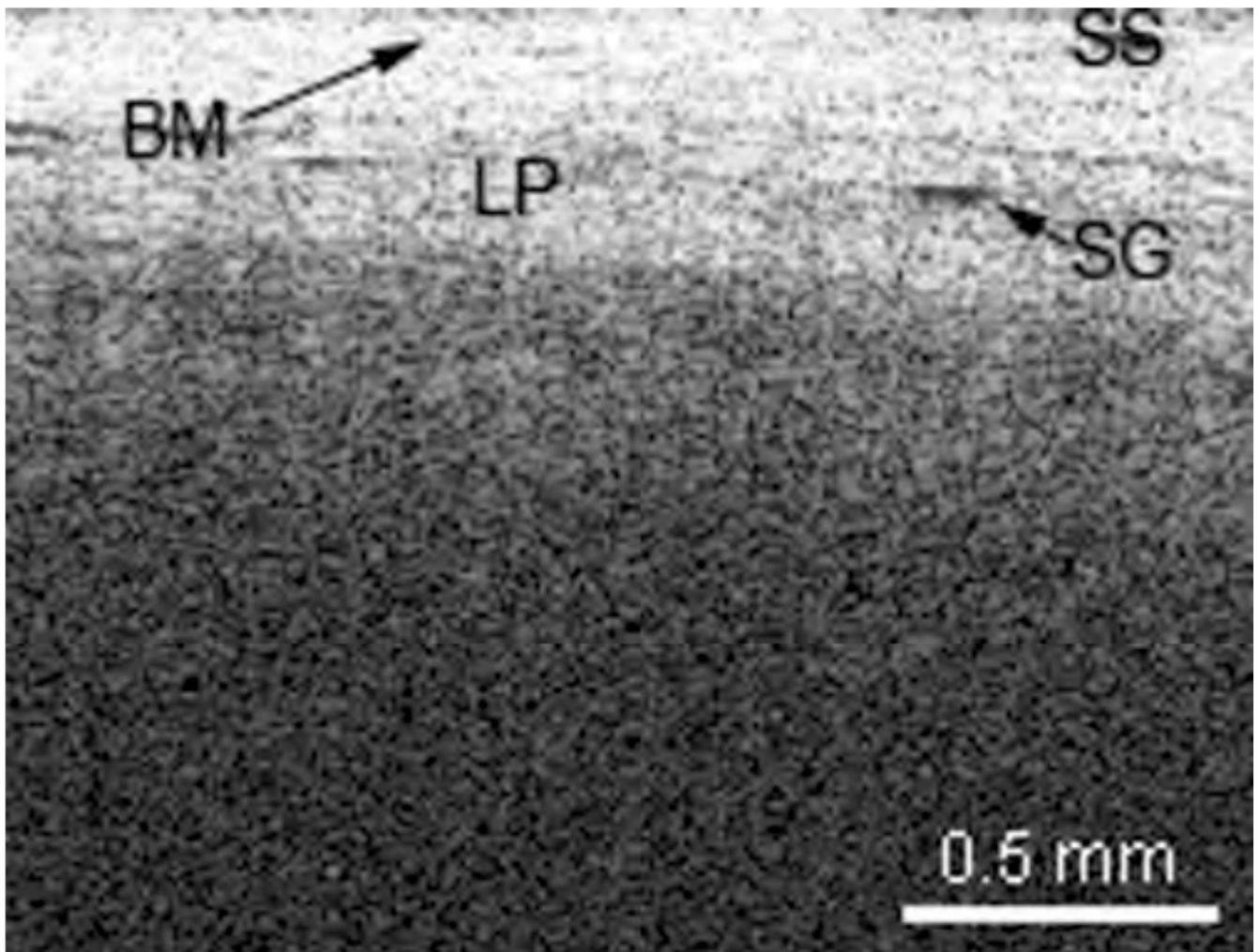


**Figure 8.** Optical coherence tomographic image of a remnant scar in the epiglottis. BM = basement membrane; LP = lamina propria; SG = seromucinous glands; SS = stratified squamous epithelium.

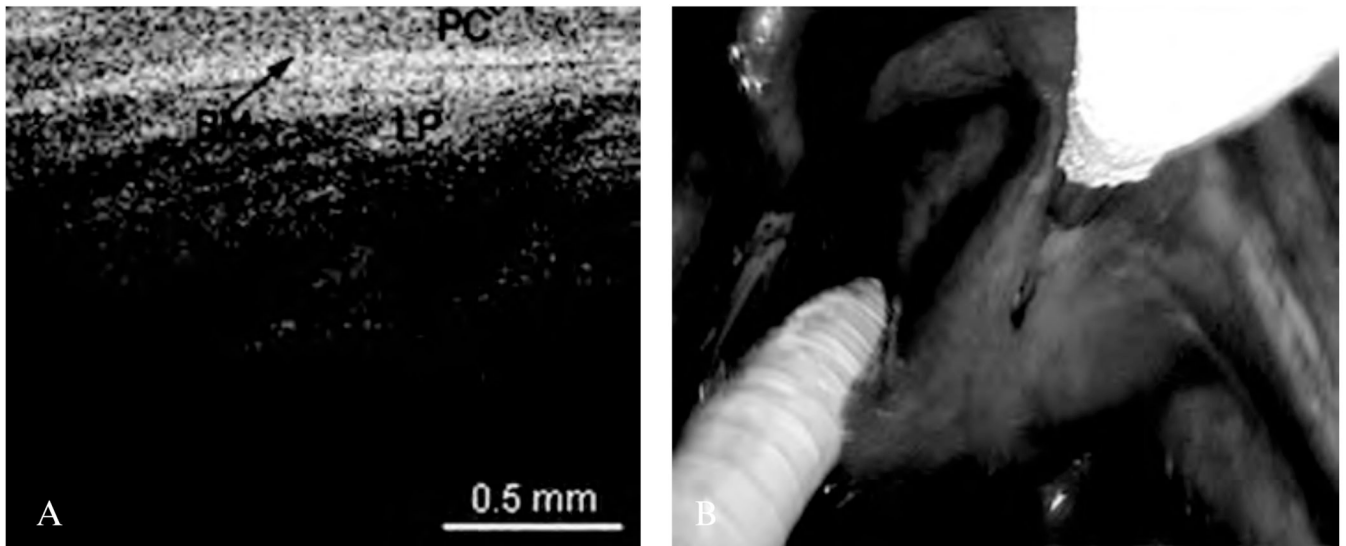


**Figure 9.**  
A, Optical coherence tomographic (OCT) image of the normal aryepiglottic fold. BM = basement membrane; LP = lamina propria; PC = pseudostratified columnar epithelium. B, Endoscopic image showing the OCT probe being placed at the aryepiglottic fold.

**Table 1**

Summary of Non-Commercially Available Optical Coherence Tomographic Systems with Higher Resolution and Scanning Rate

	<b>Jeon et al (UCI)<sup>38</sup></b>	<b>Potsaid et al (MIT)<sup>39</sup></b>	<b>Oh et al (MGH)<sup>40</sup></b>
Scanning rate	45.6 kHz	106 kHz (70–312 kHz)	50 kHz
Axial resolution	6.6 $\mu\text{m}$ (air) 4.7 $\mu\text{m}$ (tissue)	2.8 $\mu\text{m}$ (air) 2.1 $\mu\text{m}$ (tissue)	9.8 $\mu\text{m}$ (air)
Source	Fourier domain mode-locked	Spectral/Fourier domain	Fourier domain

MGH = Massachusetts General Hospital; MIT = Massachusetts Institute of Technology; UCI = University of California Irvine.